Fe-Mn cation ordering in fayalite – tephroite $(Fe_xMn_{1-x})_2SiO_4$ olivines: a neutron diffraction study

S. A. T. REDFERN

Department of Earth Sciences, University of Cambridge, Downing Street, Cambridge, CB2 3EQ, UK

K. S. KNIGHT

ISIS, Rutherford Appleton Laboratory, Oxon, OX11 0QX, UK

C. M. B. HENDERSON

Department of Earth Sciences, University of Manchester, Oxford Road, Manchester, M13 9PL, UK

AND

B. J. WOOD

Department of Geology, University of Bristol, Queens Road, Bristol, BS8 1RJ, UK

ABSTRACT

Time-of-flight neutron powder diffraction has been employed to determine precise occupancies of the M1 and M2 metal cation sites in synthetic olivines of compositions $(Fe_{0.3}Mn_{0.7})_2SiO_4$, $(Fe_{0.5}Mn_{0.5})_2SiO_4$, and $(Fe_{0.7}Mn_{0.3})_2SiO_4$. The distribution coefficient for Fe-Mn exchange in these samples has values of 4.864, 3.976, and 4.078, reflecting the preference of Mn^{2+} for the M2 site, over Fe^{2+}. These results, and the behaviour of the difference in mean bond lengths of the two sites, indicate that, while showing a tendency towards ordering, the composition-dependence of the solid solution is near ideal.

KEYWORDS: olivines, netron powder diffraction, cation sites, bond length.

Introduction

THE distribution of metal cations over the two six-fold M-sites of olivine has been the subject of intense scrutiny since the first recognition of the possibility of M-site order/disorder in this mineral (Ghose, 1962). In olivine, the two octahedral sites, denoted M1 and M2, remain symmetrically distinct at all temperatures, pressures and compositions. The M1 sites lie on 4a Wycoff positions (coinciding with a centre of symmetry and diad axis), while M2 sites are at 4c Wycoff positions (lying on mirror planes) of the *Pbnm* structure. Despite the differentiation of the two sites imposed by symmetry, metal cations are still able to disorder non-convergently between them, with a random distribution of one or more types of cation anticipated on the two sites at infinite temperature. In fact, most observations of olivines on the forsterite–fayalite join indicate that Fe and Mg are predominantly disordered at low temperatures (although fascinating ordering behaviour appears to set in on increasing temperature, but that is another story: Artioli *et al.*, 1995; Rinaldi and Wilson, 1996; Henderson *et al.*, 1996*a,b*).

It seems that the interplay of crystal field effects, ionic radius, and the degree of covalent bonding is finely balanced in Fe-Mg olivines, and hence their tendency towards M-site disorder. Other transition metals, however, show more significant inter-site partitioning. In particular, Mn-rich olivines (knebelites) tend to show preference of Mn^{2+} for the M2 site, over Fe^{2+} or Mg^{2+}, with non-convergent disordering only induced by heating to temperatures in excess of approximately 500°C (Henderson *et al.*, 1996*a,b*; Redfern *et al.*, 1996, 1997). The M-site partitioning of cations in fayalite–tephroite

olivines, the subject of this paper, can be understood simply in terms of ionic radii — the larger of the two ions (Mn^{2+}) showing preference for the larger of the two sites, M2 (Brown, 1982).

The composition-dependence of metal cation ordering in olivine was investigated for a number of cation pairs by Lumpkin and Ribbe (1983), who sought to correlate the cell parameters of olivines with their M-site occupancies and composition. At that time, the majority of determinations of olivine M-site occupancies had been made using single crystal X-ray diffraction methods. Since then Mössbauer spectroscopy has also been employed to study M-site partitioning in olivines, as have X-ray and neutron powder diffraction. Tephroite–fayalite olivines pose a particular challenge for study by X-ray diffraction, since the X-ray atomic scattering factors of Fe and Mn are nearly identical (Z_{Mn} = 26, Z_{Fe} = 27), and site occupancies cannot therefore be refined directly by X-ray diffraction. In a later paper, Miller and Ribbe (1985) attempted to identify the correlations between cell parameters and site occupancies for Fe-Mn olivines, but used the Mössbauer results of Annersten *et al.* (1984) as their data

source. Their Mössbauer study provided the first indication of the strength of preference of Mn^{2+} for M2 in these olivines. Since then, neutron scattering had been shown to be particularly valuable as a technique for determining site occupancies in this system, by virtue of the very strong neutron scattering contrast between Fe and Mn nuclei. The nuclear scattering lengths of these two atoms (assuming natural isotopic abundances) are b_{Fe} = 9.45 fm and b_{Mn} = −3.73 fm respectively (Sears, 1992), neutrons undergoing a phase change on scattering from a Mn nucleus. This strong scattering contrast means that changes in site occupancies of the M1 and M2 sites induce large changes in the intensities of certain reflections in the neutron diffraction pattern. We can see the effect of this strong scattering contrast in simulated neutron powder diffraction patterns of an olivine of composition $(Fe_{0.5}Mn_{0.5})_2SiO_4$ in which the distribution of Fe and Mn is varied from Fe being all ordered onto M1 to being all ordered onto M2 (Fig. 1).

Ballet *et al.* (1987) first demonstrated the sensitivity and utility of neutron powder diffraction in the study of the magnetic and order-disorder properties of Fe-Mn olivines, using
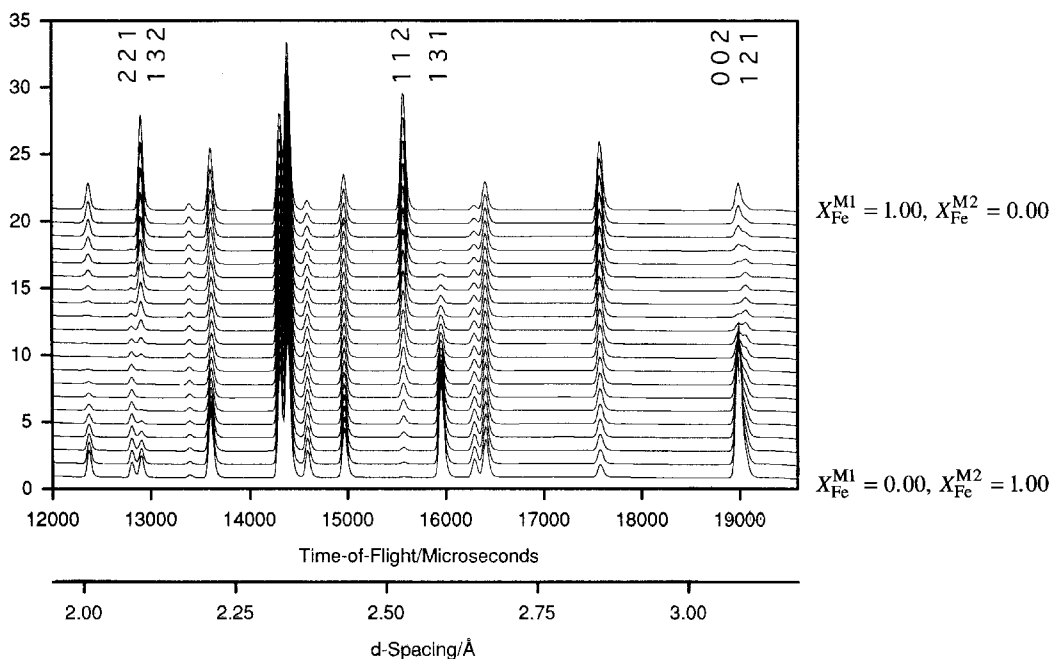

FIG. 1. Simulated neutron powder diffraction patterns of knebelites, as a function of M-site occupancy. Note the large changes in intensity of certain reflections, due to the large neutron scattering contrast between Mn and Fe.

monochromatic neutron powder diffraction at a reactor source. Their primary interest was in the nature of the low-temperature anti-ferromagnetic ordering, and unfortunately they do not report all the structural data of their refinements (they omit to report the atomic positions). We have focused specifically on the order-disorder behaviour of the solid solution in this study, and its relationship to the structure, employing time-of-flight powder diffraction techniques with polychromatic neutron radiation at the ISIS pulsed neutron spallation source, Rutherford Appleton Laboratory (England). Not only does the large scattering contrast help us in determining absolute site occupancies, the fact that the nuclear scattering length is essentially independent of scattering vector over the range of d-spacings used for structural refinement, means that useful data can be obtained down to very low d-spacings (of 0.5 Å or less). This is in contrast to X-ray diffraction, where the form factor attenuates the intensities of reflections at low d-spacings. Furthermore, detectors are arranged at high angle ($145°$) to ensure that the time-of-flight data have as high a resolution as is practicable. Thus, we are able to determine M-site occupancies in Fe-Mn olivines with high precision and accuracy. Here, we extend our earlier studies of the temperature dependent ordering of Fe and Mn in $(Fe_{0.5}Mn_{0.5})_2SiO_4$ olivine (Henderson $et\ al.$, 1996a,b; Redfern $et\ al.$, 1996, 1997) to the composition-dependent ordering of this system as observed at ambient temperature, giving the first reports of the structural response to order-disorder across the solid solution.

Experimental methods

Synthetic olivines of compositions $(Fe_{0.3}Mn_{0.7})_2SiO_4$, $(Fe_{0.5}Mn_{0.5})_2SiO_4$, and $(Fe_{0.7}Mn_{0.3})_2SiO_4$ were prepared from stoichiometric mixtures of Fe_2O_3, MnO and SiO_2. These mixtures were crystallised at 1150°C for three periods of twelve hours each in a gas-mixing furnace, buffered in a $CO-CO_2$ gas mixture at about 1 log unit more oxidising than the $Fe-FeO$ buffer. Samples were re-ground and re-homogenised between each annealing period. All samples were quenched from their final annealing period identically, in the reducing gas atmosphere. Preliminary characterisation of the run products by X-ray diffraction showed them to be homogeneous and phase pure, as was later confirmed in our neutron diffraction experiments.

Around 3.5 g of each sample was loaded into a standard vanadium sample can and mounted in the sample chamber of the POLARIS neutron time-of-flight powder diffractometer (Hull $et\ al.$, 1992). Diffraction patterns were collected over a data range of 3000 to 19600 µs, corresponding to d-spacings down to 0.5 Å, using 38 ^{3}He gas tube detectors positioned at around $2\theta = 145°$, and electronically focused and binned to provide a final diffraction pattern. Time channel binning of the data gave a resolution, dt/t, of 5×10^{-3}. Data were collected for approximately six hours, at which point subsequent refinements were not found to be limited by statistical noise in the data.

Structural data were obtained by whole pattern refinement using the Rietveld method (Rietveld, 1969), refining the structures in space group $Pbnm$ on the basis of 1878 observations. As well as 18 structural parameters (atom positions, M-site occupancies, and isotropic temperature factors) there were 3 cell parameters, 4 profile parameters and 10 background parameters (to a Chebychev polynomial) in the refinement. The effective scattering lengths for the M1 and M2 sites were refined as $X_{Mn}^{Mj}b_{Mn} + X_{Fe}^{Mj}b_{Fe}$, where X_{Mn}^{Mj} is the fractional occupancy of site M_j by Mn, etc. The total occupancies over the two M-sites were constrained to sum in agreement with the overall stoichiometry. All structures were refined to convergence.

Structural variations across the solid solution

The results of the refinements are given in Table 1. An illustration of the goodness of fit is given in Fig. 2, where the diffraction pattern of the $(Fe_{0.3}Mn_{0.7})_2SiO_4$ sample is shown together with the fit from the Rietveld refinements, and the difference between data and fit. The results for the site occupancies are given in Fig. 3, where the partitioning of Fe^{2+} between M1 and M2, as measured in this study, is compared with that obtained by Ballet $et\ al.$ (1987) and Annersten $et\ al.$ (1984). The results for site occupancies agree qualitatively with the earlier studies, highlighting the preference of Mn^{2+} for the M2 site, over Fe^{2+}. This preference is similar to that observed for Mg-Mn exchange (Brown, 1970; Francis and Ribbe, 1980; Lumpkin and Ribbe, 1983; Henderson $et\ al.$, 1996a,b; Redfern $et\ al.$, 1996, 1997), and may readily be explained in terms of ionic size criteria. While Fe^{2+} shows almost equal preference for M1 and M2 in $(Fe,Mg)_2SiO_4$ olivines, the dominant preference of Mn^{2+} for the larger M2 site drives

TABLE 1. Refined parameters of $(Fe_{0.3}Mn_{0.7})_2SiO_4$, $(Fe_{0.5}Mn_{0.5})_2SiO_4$, and $(Fe_{0.7}Mn_{0.3})_2SiO_4$. Figures in parentheses show the standard deviation (as the error in the last digit)

a. $(Fe_{0.3}Mn_{0.7})_2SiO_4$

Pbnm, R_{wp} = 1.16%, a = 4.87890(3) Å, b = 10.60587(7) Å, c = 6.20468(4) Å

Atom	x	y	z	$B_{iso}/Å^2$	site occupancy *
M1	0	0	0	0.36(5)	Fe = 0.454(2), Mn = 0.546(2)
M2	0.9954(8)	0.2793(4)	1/4	0.54(6)	Fe = 0.146(2), Mn = 0.854(2)
Si	0.4285(3)	0.0960(1)	1/4	0.39(2)	
O1	0.7606(3)	0.0926(1)	1/4	0.68(2)	
O2	0.2126(3)	0.4536(1)	1/4	0.62(2)	
O3	0.2871(2)	0.1637(1)	0.0395(1)	0.58(1)	

b. $(Fe_{0.5}Mn_{0.5})_2SiO_4$

Pbnm, R_{wp} = 1.36%, a = 4.86184(4) Å, b = 10.58358(9) Å, c = 6.16950(5) Å

Atom	x	y	z	$B_{iso}/Å^2$	site occupancy *
M1	0	0	0	0.41(2)	Fe = 0.666(2), Mn = 0.334(2)
M2	0.9786(3)	0.2824(9)	1/4	0.41(2)	Fe = 0.334(2), Mn = 0.666(2)
Si	0.4281(4)	0.0961(2)	1/4	0.36(3)	
O1	0.7636(3)	0.0922(1)	1/4	0.62(2)	
O2	0.2132(3)	0.4536(1)	1/4	0.60(3)	
O3	0.2876(2)	0.1638(1)	0.0384(2)	0.59(2)	

c. $(Fe_{0.7}Mn_{0.3})_2SiO_4$

Pbnm, R_{wp} = 1.75%, a = 4.84857(3) Å, b = 10.55545(7) Å, c = 6.14054(4) Å

Atom	x	y	z	$B_{iso}/Å^2$	site occupancy *
M1	0	0	0	0.51(1)	Fe = 0.839(2), Mn = 0.161(2)
M2	0.9845(6)	0.2804(2)	1/4	0.40(1)	Fe = 0.561(2), Mn = 0.439(2)
Si	0.4292(4)	0.0966(2)	1/4	0.39(2)	
O1	0.7657(3)	0.0924(2)	1/4	0.64(2)	
O2	0.2124(3)	0.4535(1)	1/4	0.62(2)	
O3	0.2875(2)	0.1643(1)	0.0381(2)	0.58(1)	

* blank if site fully occupied.

Fe^{2+} into M1 in fayalite-tephroite olivines. The iron-manganese distribution is discussed in greater detail below.

The effect of changing composition across the solid solution is reflected in variations in the cell parameters and the sizes and shapes of the coordination polyhedra. The cell-parameter variation, shown as a function of composition across the solid solution, is given in Fig. 4, where our results are compared with those of Ballet *et al.* (1987) and Annersten *et al.* (1984). We see appreciable curvature of the b cell parameter in

particular, which is interesting because Fe-Mn exchange occurs between octahedra in the [010] direction, the curvature in the cell parameter resulting from ordering of the cations between M1 and M2, and the cell parameter reaching a maximum at 70 mol % tephroite.

The behaviour of the M1−O and M2−O bond lengths is shown as a function of composition in Fig. 5, and all bond lengths are listed in Table 2. The principal effect of substituting Mn for Fe is to increase the size of both octahedra, as might be expected given each contains some Mn, and as can
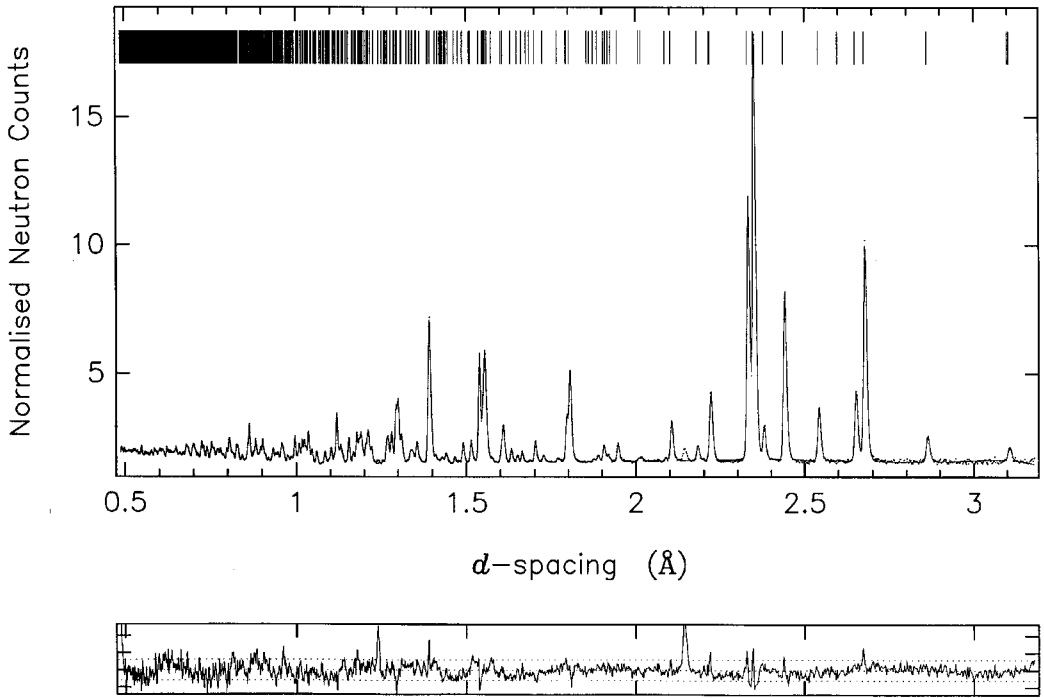
FIG. 2. Time-of-flight neutron powder diffraction pattern of $(Fe_{0.3}Mn_{0.7})_2SiO_4$. Vertical bars represent the positions of reflections. The solid line is the Rietveld fit to the data. The difference between fit and experiment is shown in the lower part of the figure.
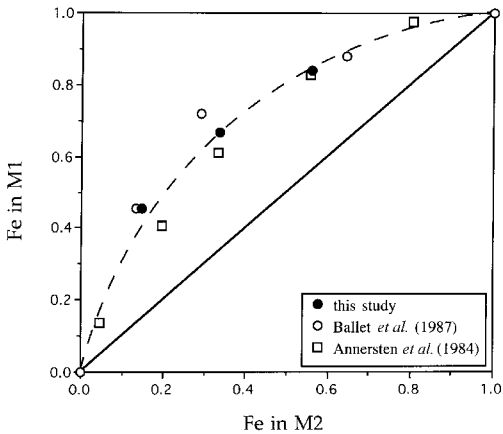

FIG. 3. Iron site occupancy in $(Fe_xMn_{1-x})_2SiO_4$ olivines. The straight line shows the behaviour of a disordered solid solution ($K_D = 1$), while the dashed line shows the behaviour of a partially ordered solid solution with K_D ≈ 4. Solid circles: this study. Open circles: Ballet *et al.* (1987). Open squares: Annersten *et al.* (1984).

be seen from the mean M-O bond lengths at both sites, shown in Fig. 6. Within the M2 octahedron, significantly non-linear behaviour is seen for the M2–O3a and M2–O3b bond lengths, which appear to be sensitive to the degree of order. In fact, reviewing the data of Redfern *et al.* (1997), for the high-temperature behaviour of the related olivine, $(Mg_{0.5}Mn_{0.5})_2SiO_4$, we see that the changes at the M2 site with changes in degree of M1-M2 order can be substantial. On heating, the $(Mg_{0.5}Mn_{0.5})_2SiO_4$ sample began to disorder at temperatures above 600°C (Redfern *et al.*, 1997). We see from the bond lengths of the M2 site that, at the same temperature, the M2–O3a and M2–O3b bond lengths begin to become more alike (Fig. 7). Upon disordering at high-temperature, the M2 site changes from appearing to be trigonally distorted to appearing tetragonally distorted. Generalising from the results of the high-temperature study, one might conclude that the effect of ordering on the M2–O bond lengths is, therefore, to make M2–O3a and
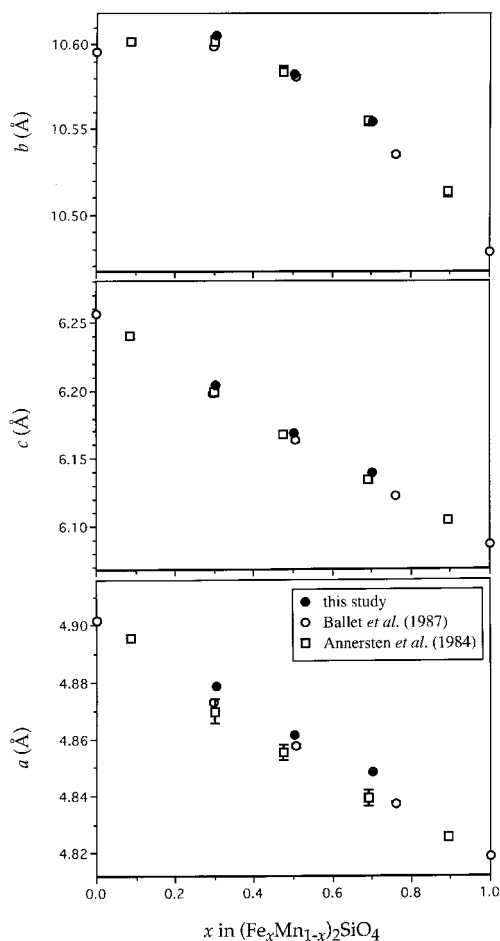
FIG. 4. Cell parameters of $(Fe_xMn_{1-x})_2SiO_4$ olivines, as a function of composition. Solid circles are the results of this study, open circles are data from the neutron diffraction study of Ballet *et al.* (1987), and open squares are data from Annersten *et al.* (1984). Where error bars are not shown, the errors are smaller than the size of the symbols.

FIG. 5. $M-O$ bond lengths in $(Fe_xMn_{1-x})_2SiO_4$ olivines as a function of composition. Data for Fe_2SiO_4 and Mn_2SiO_4, shown as crosses, are from Fujino *et al.* (1981).

M2−O3b more dissimilar from one another. Comparing these observations with the results for our $(Fe_xMn_{1-x})_2SiO_4$ samples (Fig. 5), we see that the variation in M2−O bond lengths across the solid solution might suggest that the system is displaying more order at intermediate compositions. We shall see, however, that the refined site occupancies of the M1 and M2 sites do not bear this conclusion out, which indicates that th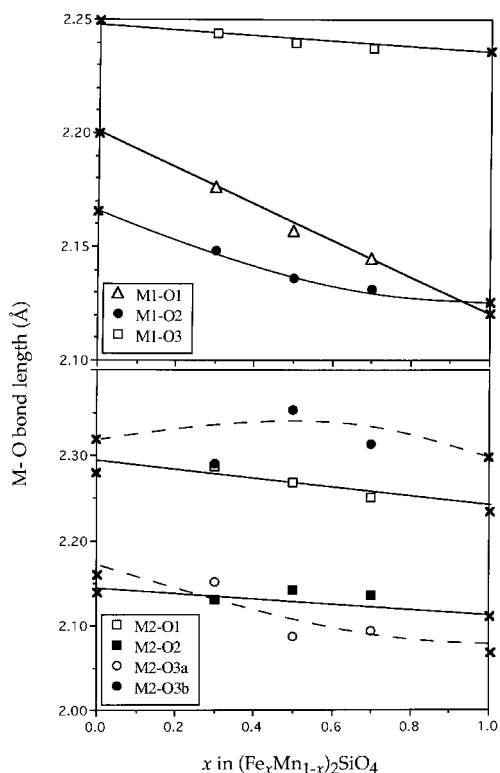e compositional controls on the bond lengths may not fully reflect the effects induced by temperature. We note, however, that the temperature-dependent behaviour of the bond lengths at the M2 site in $(Mg_{0.5}Mn_{0.5})_2SiO_4$ (Fig. 7) indicate that the local strains associated with order-disorder in these systems can be quite considerable: there is approximately 5% change in bond lengths between 600°C and 1250°C, over which temperature range there are changes in the degree of M1−M2 order from around 35% ordered to 25 % ordered.

Iron−manganese distribution in olivine

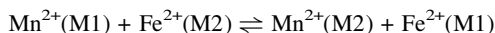The intracrystalline exchange of Mn^{2+} and Fe^{2+} may be expressed in terms of the following reaction:

$$Mn^{2+}(M1) + Fe^{2+}(M2) \rightleftharpoons Mn^{2+}(M2) + Fe^{2+}(M1)$$

TABLE 2. Bond lengths (Å) in $(Fe_{0.3}Mn_{0.7})_2SiO_4$, $(Fe_{0.5}Mn_{0.5})_2SiO_4$, and $(Fe_{0.7}Mn_{0.3})_2SiO_4$. Figures in parentheses show the standard deviation (as the error in the last digit)

	$(Fe_{0.3}Mn_{0.7})_2SiO_4$	$(Fe_{0.5}Mn_{0.5})_2SiO_4$	$(Fe_{0.7}Mn_{0.3})_2SiO_4$
M1–O1 ($\times$ 2)	2.176 (1)	2.157 (1)	2.144 (1)
M1–O2 ($\times$ 2)	2.148 (1)	2.136 (1)	2.131 (1)
M1–O3 ($\times$ 2)	2.244 (1)	2.240 (1)	2.237 (1)
M2–O1 ($\times$ 1)	2.288 (4)	2.267 (1)	2.250 (3)
M2–O2 ($\times$ 1)	2.131 (4)	2.141 (1)	2.135 (3)
M2–O3a ($\times$ 2)	2.151 (2)	2.086 (3)	2.094 (2)
M2–O3b ($\times$ 2)	2.288 (3)	2.353 (6)	2.314 (2)
Si–O1 ($\times$ 1)	1.621 (2)	1.632 (2)	1.632 (2)
Si–O2 ($\times$ 1)	1.660 (2)	1.657 (2)	1.659 (2)
Si–O3 ($\times$ 2)	1.642 (1)	1.638 (2)	1.636 (2)

which, assuming ideality, has the equilibrium constant:

$$K_D = \frac{x_{Fe}^{M1}(1 - X_{Fe}^{M2})}{(1 - X_{Fe}^{M1})X_{Fe}^{M2}}$$

which is the distribution coefficient for intracrystalline partitioning over the two sites. Thus, $K_D = 1$ implies complete disorder over M1 and M2, $K_D = 0$ implies complete anti-order (that is, the larger cation (Mn) entering the smaller site (M1)) and $K_D = \infty$ implies complete order. The distribution coefficient for Fe-Mn exchange in our samples

takes the values of 4.86 ± 0.07, 3.98 ± 0.06, and 4.08 ± 0.06 for $(Fe_{0.3}Mn_{0.7})_2SiO_4$, $(Fe_{0.5}Mn_{0.5})_2SiO_4$, and $(Fe_{0.7}Mn_{0.3})_2SiO_4$ respectively. This demonstrates the near ideality of the solid solution; the tendency to order is dependent upon temperature, not upon composition, and the degree of order as a function of composition is approximately constant. The average value of our three samples is $K_D = 4.31 \pm 0.05$. This compares with the average value of 3.8 determined by Annersten *et al.* (1984) using Mössbauer
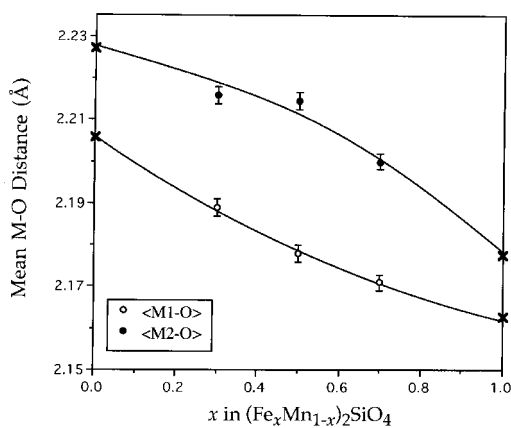

FIG. 6. Mean M–O bond lengths in $(Fe_xMn_{1-x})_2SiO_4$ olivines as a function of composition. Data for Fe_2SiO_4 and Mn_2SiO_4, shown as crosses, are from Fujino *et al.* (1981).
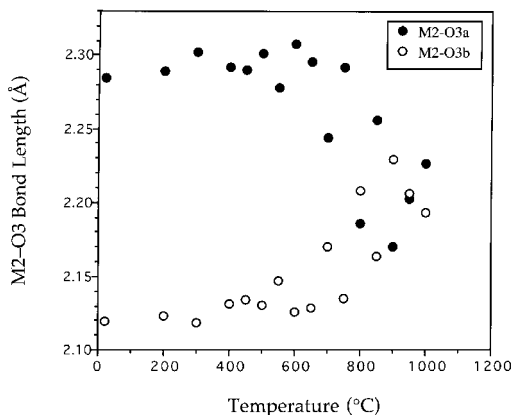

FIG. 7. M2–O3 bond lengths in $(Mg_{0.5}Mn_{0.5})_2SiO_4$ olivine as a function of temperature (from the data of Redfern *et al.*, 1997). Upon heating, this sample disordered at temperatures above 600°C. The effect of temperature-induced disordering is to make the M2–O3a and M2–O3b bond lengths more alike.

spectroscopy. They assumed that this corresponded to the equilibrium distribution of the sample, quenched from its annealing temperature (their samples were annealed at 1000°C). Since configurational disorder increases with temperature, we would expect $K_{D,T\,=\,1000°C} > K_{D,T\,=\,1150°C}$, rather than the relationship suggested by the data. The slight discrepancy may arise from the fact that neither our value of $\langle K_D \rangle = 4.31$ nor the value of K_D obtained by Annersten *et al.* (1985) represents the true equilibrium state of order of samples quenched in from their annealing temperatures. Indeed, Redfern *et al.* (1997) have shown that the value of K_D measured at room temperature is highly sensitive to the quench rate from the conditions of annealing. The *in situ* high-temperature results of Redfern *et al.* (1996) show that, in this case, our value of $K_D = 4.31$ corresponds to a fictive equilibrium temperature of approximately 880 K, and a rather slow quench rate, whereas the value of $K_D = 3.8$ obtained by Annersten *et al.* (1985) corresponds to a fictive equilibrium temperature of around 980 K and a quench rate approximately 10 times faster. This may be a consequence of the difference in size between our rather large ceramic pressed samples (as required for neutron work) and Annersten *et al.*'s smaller Mössbauer samples. We also note that our results suggest that K_D is largely independent of composition (and that the solid solution is very near ideal). The small (but admittedly significant) differences in our values of K_D could be ascribed to the three samples having experienced slightly different cooling rates on quenching. The results of Annersten *et al.* (1984) gave a very large sample-to-sample variation in K_D (ranging from 2.76 to 9.85), which is in marked contrast to our results. We suspect that this variation within their data-set reflects more substantial differences in the quench rates for their samples, and is an experimental artefact, since it is not correlated with the compositional variations in their samples.

Acknowledgements

References

Annersten, H., Adetunji, J. and Filippidis, A. (1984) Cation ordering in Fe-Mn silicate olivines. *Amer. Mineral.*, **69**, 1110−5.

Artioli, G., Rinaldi, R., Wilson, C.C. and Zanazzi, P.F. (1995) High-temperature cation partitioning in olivine: In situ single-crystal neutron diffraction study. *Amer. Mineral.,* **80**, 197−200.

Ballet, O., Fuess, H. and Fritzsche, T. (1987) Magnetic structure and cation distribution in $(Fe,Mn)_2SiO_4$ (olivine) by neutron diffraction. *Phys. Chem. Minerals*, **15**, 54−8.

Brown, G.E. (1982) Olivine and silicate spinels. In *Orthosilicates* (P.H. Ribbe, ed.). *Reviews in Mineralogy*, **5**, 2nd edition, p. 275−381. Mineralogical Society of America, Washington, D.C.

Francis, C. A. and Ribbe, P.H. (1980) The forsterite–tephroite series: 1. Crystal structure refinements. *Amer. Mineral.,* **65**, 1263−9.

Fujino, K., Sasaki, S., Takéuchi, Y. and Sadanaga, R. (1981) X-ray determination of electron distributions in forsterite, fayalite and tephroite. *Acta. Crystallogr.*, **B37**, 513−8.

Ghose, S. (1962) The nature of Mg^{2+}-Fe^{2+} distribution in some ferromagnesian silicate minerals. *Amer. Mineral.*, **47**, 388−94.

Henderson, C.M.B., Artioli, G., Knight, K.R., Redfern, S.A.T., Rinaldi, R. and Wood, B.J. (1996*a*) Temperature and composition dependenc of Fe-Mg ordering in olivines. ISIS 1996 Annual Report (CLRC), A18.

Henderson, C.M.B., Knight, K.S., Redfern, S.A.T. and Wood, B.J. (1996*b*) High-temperature study of octahedral cation exchange in olivine by neutron powder diffraction. *Science*, **271**, 1713−5.

Hull, S., Smith, R.I., David, W.I.F., Hannon, A.C., Mayers, J. and Cywinski, R. (1992) The POLARIS powder diffractometer at ISIS. *Physica B*, **180**, 1000−2.

Lumpkin, G.R. and Ribbe, P.H. (1983) Composition, order-disorder and lattice parameters of olivines: relationships in silicate, germanate, beryllate, phosphate and borate olivines. *Amer. Mineral.*, **68**, 164−76.

Miller, M.L. and Ribbe, P.H. (1985) Methods for determination of composition and intracrystalline cation distribution in Fe-Mn and Fe-Ni silicate olivines. *Amer. Mineral.*, **70**, 723−8.

Redfern, S.A.T., Henderson, C.M.B., Wood, B.J., Harrison, R.J. and Knight, K.S. (1996) Determination of olivine cooling rates from metal-cation ordering. *Nature*, **381**, 407−9.

Redfern, S.A.T., Henderson, C.M.B., Knight, K.S. and Wood, B.J. (1997) High-temperature order-disorder in $(Fe_{0.5}Mn_{0.5})_2SiO_4$ and $(Mg_{0.5}Mn_{0.5})_2SiO_4$ olivines: an in situ neutron diffraction study. *Eur. J. Mineral.*, **9**, 287−300.

Rietveld, H.M. (1969) A profile refinement methods for nuclear and magnetic structures. *J. Appl.*

Crystallogr., **2**, 65−71.

Rinaldi, R. and Wilson, C.C. (1996) Crystal dynamics by neutron time-of-flight Laue diffraction in olivine up to 1573 K using single frame methods. *Solid State Comm.*, **97**, 395−400.

Sears, V.F. (1992) Neutron scattering lengths and cross sections. *Neutron News*, **3**, 26−37.